THE ASTROPHYSICAL JOURNAL, 180:207–225, 1973 February 15

ROTATING MAGNETOSPHERE: A SIMPLE RELATIVISTIC MODEL

F. CURTIS MICHEL
Institute for Theoretical Astronomy, Cambridge, England, and
Space Science Department,* Rice University
Received 1972 July 31

ABSTRACT

We solve exactly for the electromagnetic field configuration about an aligned rotating magnetic moment ("star") for the case that there is sufficient plasma about the object to "freeze in" the magnetic fields, but in the limit that the inertia and pressure of the plasma particles can be neglected. These solutions are expected to be valid except near the light cylinder, although there is no *mathematical* difficulty in solving the resultant equations at or even beyond the light cylinder. The solutions show quantitatively how the field lines make the transition from a closed (dipole-like) to an open configuration and provide a refined estimate of how much magnetic flux is available to open field lines (an important point in many pulsar theories). We find that if a flux Φ from an unperturbed dipole closes outside the light cylinder, then for the perturbed field this flux is increased by a factor of about 1.592. The field lines in the dipole case exhibit a cusp at the light cylinder, and we can calculate the charge density there. This charge density is found to be insufficient to account for coherent radiation of radiofrequency waves from pulsars.

Subject headings: hydromagnetics — magnetic stars — pulsars — relativity — rotation, stellar

I. INTRODUCTION

There has been considerable interest in the properties of rapidly rotating magnetized stars, particularly given the now popular expectation that pulsars are such objects. One would like to have models for such objects that are analytically tractable on the one hand but physically interesting on the other. Insofar as model building goes, there are two major decisions: (1) what magnetic field configuration to assume, and (2) how much plasma to put around the object. Note that we are not at this point trying to model pulsars per se; otherwise questions such as "What is the emission mechanism?" etc., would have priority.

Our first decision is dictated by logic, namely, to examine the simplest case first, which is to take the magnetic field to be an axisymmetric magnetic multipole with the symmetry axis coincident with the rotation axis. We will find that the multipolarity or combination of multipolarities makes relatively little difference, and can be handled with the techniques developed here.

The second decision is to consider the case with enough charged particles around to constitute a plasma. It is well known (Ferraro 1937) that plasma around a rotating magnetized conducting body corotates with the body. This result depends on there being electrical contact with the body, since the rotating body develops potential differences and if the plasma is not at first corotating with it, currents flow that act to slow the body and accelerate the plasma toward corotation. On the other hand, corotation cannot be maintained beyond the distance at which the velocity of light would be exceeded (the "light cylinder"). As the light cylinder is approached, the centrifugal force exerted by the plasma increases whereas the magnetic field decreases with increased distance from the source. At some point within the light cylinder the plasma forces overcome the magnetic field and the field lines should be pulled open. It would be interesting to calculate where such a transition takes place, but that must

* Permanent address.

depend on the field strength and plasma density. However, we can (and will) avoid confronting directly the problem of handling plasma inertia by considering the artificial case of a plasma of charged particles having arbitrarily small but nonzero mass. In this way we propose to asymptotically approach the light cylinder. The assumption of negligible particle mass is equivalent to the assumption of an arbitrarily strong magnetic field. A certain minimum plasma concentration is necessary to provide the space charge and current distribution required for corotation; however, this concentration is proportional to the field magnitude B, whereas the restoring forces are proportional to B^2.

II. EQUATIONS

The resulting equations are quite simple. We have on the one hand the frozen-in-flux condition,

$$\boldsymbol{E} + \boldsymbol{V} \times \boldsymbol{B} = 0 ; \tag{1}$$

and on the other the force balance equation,

$$j_0 \boldsymbol{E} + \boldsymbol{j} \times \boldsymbol{B} = \text{inertial terms} \to 0 , \tag{2}$$

where j_0 is the charge density and $\boldsymbol{j}$ is the current density. If particle mass and pressure were included, equation (1) would hold only approximately since then other forces would cause particle drifts, and the inertial terms would not be zero in equation (2). Multiplying equation (1) by j_0 and subtracting gives

$$(j_0 \boldsymbol{V} - \boldsymbol{j}) \times \boldsymbol{B} = 0 ; \tag{3}$$

thus

$$\boldsymbol{j} = j_0 \boldsymbol{V} + \text{component parallel to } \boldsymbol{B} . \tag{4}$$

In our system of equations the current component parallel to $\boldsymbol{B}$ is unspecified and, if we only consider axisymmetric fields, can be set to zero. Again, if particle inertia is included, the field lines must lag the corotation (cf. Michel 1969) and consequently currents parallel to $\boldsymbol{B}$ can and must flow. We therefore have, for zero parallel current,

$$\boldsymbol{j} = j_0 \boldsymbol{V} , \tag{5}$$

and the divergence of equation (1) gives in turn

$$j_0/\epsilon_0 + \boldsymbol{B} \cdot (\nabla \times \boldsymbol{V}) - j_0 \mu_0 V^2 = 0 , \tag{6}$$

or, rewriting to solve for j_0 and multiplying by $\mu_0 \boldsymbol{V}$ gives

$$\mu_0 \boldsymbol{j} = - \boldsymbol{V} (\boldsymbol{B} \cdot \boldsymbol{S}) / (c^2 - V^2) , \tag{7}$$

where $\boldsymbol{S} = \nabla \times \boldsymbol{V}$. What has happened is the following: corotation in a magnetic field requires a certain electric field to be present; and although the magnetic field might be a vacuum field, the required electric field is not in general a vacuum field. Thus the plasma must then provide a nonzero space charge j_0, but in turn the corotation carries the plasma (and space charge) along with velocity $\boldsymbol{V}$ to form a current $j_0 \boldsymbol{V}$. This current modifies the magnetic field, which in turn modifies the electric field, etc., and equation (7) represents the self-consistent current that must flow. From equation (7) all other quantities (j_0, $\boldsymbol{E}$, $\boldsymbol{B}$) can be derived.

Notice that $\boldsymbol{j}$ becomes infinite at the light cylinder unless $\boldsymbol{B}\cdot\boldsymbol{S}$ vanishes. For corotation,

$$\boldsymbol{V} = \omega\rho\boldsymbol{e}_\theta \tag{8}$$

in cylindrical coordinates (ρ, z, θ); hence

$$\boldsymbol{S} = 2\omega\boldsymbol{e}_z\,, \tag{9}$$

and we see that to avoid a divergence one requires that $\boldsymbol{B}$ be parallel to the equatorial plane at the light cylinder. It is just this special solution, which passes smoothly through the light cylinder, that we will examine here.

III. FIELD-LINE DESCRIPTION

There are a number of ways of reformulating equation (7), and the way we will choose is to write the field in terms of the field lines $f(\rho, z) =$ constant, in which case

$$\boldsymbol{B} = (\nabla f) \times \boldsymbol{\beta}\,, \tag{10}$$

where

$$\boldsymbol{\beta} = \boldsymbol{e}_\theta/\rho\,. \tag{11}$$

Here f and β may be recognized as essentially Euler potentials chosen such that f labels each field line in the case of symmetry about the $z =$ axis. The significance of f follows immediately simply by evaluating equation (10), in which case we find

$$B_\rho = -f_z/\rho\,, \tag{12a}$$

$$B_z = f_\rho/\rho\,, \tag{12b}$$

where $f_z = \partial f/\partial z$, etc. The curl of $\boldsymbol{B}$ is simply

$$\mu_0\boldsymbol{j} = -(f_{\rho\rho} + f_{zz})/\rho + f_\rho/\rho^2\,; \tag{13}$$

but from equation (7) we also have

$$\mu_0\boldsymbol{j} = -2\omega^2\rho f_\rho/(c^2 - \omega^2\rho^2)\,. \tag{14}$$

Eliminating between equations (13) and (14) then gives us

$$f_{\rho\rho} + f_{zz} - \frac{1}{\rho}\left(\frac{1+\rho^2}{1-\rho^2}\right)f_\rho = 0\,, \tag{15}$$

where z and ρ are now dimensionless lengths in units of c/ω. Equation (15) is our fundamental equation for corotating field lines. We note that (15) is linear in f, separable, and that for $\rho^2 \ll 1$ the solutions are the usual point-source multipoles for the vacuum field. The solution for a monopole, for example, is

$$f_0 = A + Bz/r\,, \tag{16}$$

where A and B are arbitrary constants, $r^2 = z^2 + \rho^2$ and f_n is the nth multipole. Higher multipoles can be obtained simply by taking multiple partial differentials of f_0 with respect to z. Thus,

$$f_1 = B\rho^2/r^3\,, \tag{17}$$

etc. Consequently we need only to solve for the monopole case, and all other axisymmetric solutions can be derived therefrom. For the monopole, we have the boundary conditions

$$f_0(z, 0) = A \pm B \qquad (z > 0, z < 0), \tag{18}$$

$$f_0(0, \rho) = A \qquad (\rho > 0), \tag{19}$$

$$\lim_{z\to\infty} f_0(z, \rho) \to A \pm B \qquad (1 \geq \rho \geq 0), \tag{20}$$

and

$$(\partial f_0/\partial \rho)_{\rho=1} = 0. \tag{21}$$

The first two are imposed by the symmetry of the monopole solution, while the third represents the decline of magnetic flux with distance (essentially a restatement of the first), and the fourth is the requirement that there be no divergence of the light cylinder. The solutions inside the light cylinder are therefore independent of those outside, and we need not be concerned therefore with that "unphysical" region (only if we interpret $\boldsymbol{j}/j_0$ as being the physical velocity of particles does the system of eqs. [1] and [2] fail: one could instead assign arbitrary $\boldsymbol{j}$ and j_0 ratios to an anisotropic medium to otherwise satisfy those equations—e.g., built up of charged superconducting loops insulated from one another—in which case the external solutions would be entirely acceptable). The value of f also has a physical significance beyond simply labeling field lines:

$$\Phi = 2\pi(f_b - f_a) \tag{22}$$

is the net magnetic flux contained between the two adjacent field lines, f_a and f_b; thus f is the magnetic flux referenced to some surface in the system. For the choice

$$A = -B = 1, \tag{23}$$

f_0 is the flux measured from the $+z$ axis.

It is straightforward to infer from the boundary conditions what shape the overall field line configuration must have, as shown in figure 1. Of particular interest is the dipole case where the line labeled $f_{\rm crit}$ in figure 1*b* forms a cusp at the light cylinder. This field line does not violate the requirement $f_\rho = 0$ at the light cylinder because $f_z = 0$ also. Thus the field strength is zero where the field line $f_{\rm crit}$ crosses the light cylinder at an angle other than 90° in the meridional (ρ, z) plane. Indeed, by expanding equation (15) about the cusp point (0, 1), we find that

$$2f_{\rho\rho} = -f_{zz} \qquad \text{(at cusp)}; \tag{24}$$

thus the angle α is $\sin^{-1}(1/\sqrt{3}) = 35.^\circ27\ldots$. This relatively narrow angle indicates how strongly the magnetic field has been distorted.

IV. SEPARATION OF VARIABLES

Equation (15) is linear and separable, and we can therefore write

$$f(z, \rho) = F(z)\psi(\rho), \tag{25}$$

where

$$F_{zz} = \lambda^2 F \tag{26}$$

and

$$\psi_{\rho\rho} - \frac{1}{\rho}\left(\frac{1 + \rho^2}{1 - \rho^2}\right)\psi_\rho = -\lambda^2\psi. \tag{27}$$

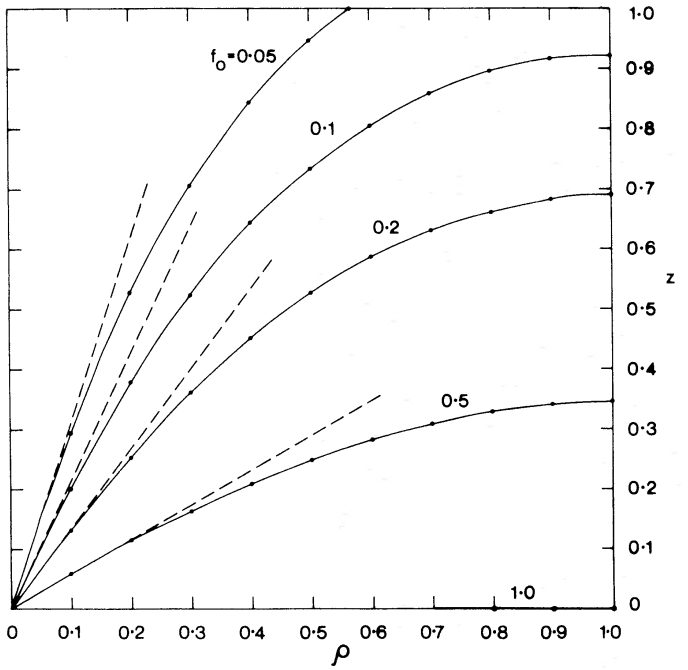

FIG. 1.—(*a*) Monopole field lines as distorted by corotation. The dashed lines show the nonrotating monopole field for the same values of the field line label, f_0, being given from $f_0 = 1 - z/r$.

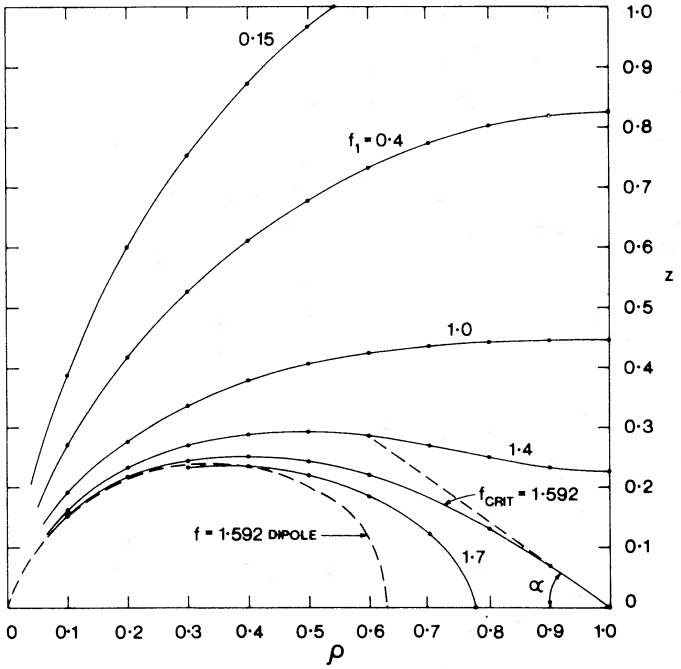

FIG. 1.—(*b*) Dipole field lines as distorted by corotation. The line $f_{\rm crit} = 1.592$ shows the field line leading to the cusp at $z = 0$, $\rho = 1$. For comparison is the same field line (*dashed*) for a vacuum dipole. The line $f_{\rm crit}$ makes an angle $\alpha = \tan^{-1}(\frac{1}{2}\sqrt{2})$ with the ρ = axis, and the extension of this field line is also shown dashed. The dots are at computed positions for the indicated values of f, using 10 eigenfunctions and the convergence techniques discussed in the text and in Appendix B. It is interesting to note how close to the origin one can approach, using such a truncated eigenvalue expansion. The solid lines are simply smooth curves drawn through the dots.

Thus

$$F = \text{const.} \times e^{-\lambda z}, \tag{28}$$

and the functions ψ are discussed in detail in Appendix A. For our purposes here let us just say that they have the properties

$$\psi(\rho) \to 0 \qquad \text{as } \rho^2 \qquad \text{for } \rho \to 0, \tag{29}$$

$$\to \text{constant} \qquad \text{for } \rho \to 1, \tag{30}$$

$$\psi_\rho(\rho) \to 0 \qquad \text{as } 1 - \rho \qquad \text{for } \rho \to 1, \tag{31}$$

but only for discrete values of λ, namely, the eigenvalues λ_n. A conjugate set of functions $\phi(\rho)$ can be defined which have the opposite boundary value behaviors [e.g., $\phi(0) =$ nonzero constant]. For each eigenvalue λ_n there is a distinct eigenfunction ψ_n. The ψ_n are orthogonal and satisfy the orthonormalization condition

$$\int_0^1 \psi_n \psi_m g d\rho = \delta_{nm} h_n, \tag{32}$$

where $g = (1 - \rho^2)/\rho$.

Note that this separation into an eigenstate expansion is exactly parallel to the analogous solution for the problem of a charged particle in a conducting cylinder. In that problem the ψ_n are Bessel functions. We then have that in general

$$f_0(z, \rho) = \sum_{n=1}^{\infty} w_n \exp(-\lambda_n z)\psi_n(\rho) \qquad (z > 0), \tag{33}$$

where w_n are constant coefficients. This expansion satisfies our boundary conditions (18), (20), and (21), leaving only $f_0(0, \rho) = 1$. From the orthonormality relation (32) we have, after multiplying by ψ_m and integrating over $g d\rho$,

$$h_m w_m = \int_0^1 \psi_m g d\rho; \tag{34}$$

and from Appendix A, we can also write this relation as

$$h_m w_m = \phi_m(0)/\lambda_m. \tag{35}$$

Returning to equation (33), we finally have

$$f_0(z, \rho) = \sum_{n=1}^{\infty} \phi_n(0) \exp(-\lambda_u z)\psi_n(\rho)/\lambda_n h_n. \tag{36}$$

The problem of calculating the eigenfunctions, eigenvalues, and normalization integrals is treated in Appendix A. The problem of obtaining acceptable accuracy without unreasonable computational effort is discussed in the next section.

V. CALCULATION OF THE CUSP BEHAVIOR OF f

The dipole case is given, as mentioned previously, simply by differentiating with respect to z; thus (remember, $B = -1$)

$$f_1(z, \rho) = \sum_{n=1}^{\infty} e^{-\lambda_n z}\psi_n(\rho)\phi_n(0)/h_n, \tag{37}$$

$$\to \rho^2/r^3 \qquad \text{as } r \to 0,$$

and thus the critical field line leading to the cusp is given by

$$f_{\rm crit} \equiv f_1(0, 1) = \sum \psi_n(1)\phi_n(0)/h_n \,. \tag{38}$$

Before calculating $f_{\rm crit}$, we will check to see how closely we can reproduce the value of $f_0(0, 1) = 1$, namely,

$$\begin{aligned} f_0(0, 1) &= \sum \psi_n(1)\phi_n(0)/\lambda_n h_n \\ &= 1\ (?)\,. \end{aligned} \tag{39}$$

If we substitute in the asymptotic (large n) expressions obtained in Appendix A, we obtain

$$f_0(0, 1) \approx -(\pi/\sqrt{2}) \sum_{n=1}^{\infty} (-1)^n \,. \tag{40}$$

Although the sum is formally nonconvergent, we recognize that taking ρ to be slightly less than unity produces convergence since ψ drops steeply from $\psi(1)$ at large values of n. Thus we can take the sum to be the Abel sum,

$$\sum_{n=1}^{\infty} (-1)^n = -\tfrac{1}{2} \,, \tag{41}$$

giving altogether

$$f_0(0, 1) \approx \pi/\sqrt{8} = 1.11\ldots \qquad \text{(asymptotic)}\,, \tag{42}$$

and we see that the asymptotic relations already come within 11 percent of the desired result. (The concern here is that one might have a Gibbs's phenomenon at $\rho = 1$.) The value of the sum can be improved by replacing the low-value n terms with their numerically determined values. In other words, we could calculate

$$f_0(0, 1) = \pi/\sqrt{8} + \sum [\psi_n(\text{exact}) - \psi_n(\text{asymp.})]\phi_n(0)/h_n\lambda_n \,,$$

and truncate the latter series once (and if) the desired accuracy can be obtained. Unfortunately, convergence is rather slow with, say, 10 terms giving an accuracy of only a few points in 10^2 and improving at a decreasing rate as more terms are added. Instead, we have used a weighting technique which produces maximum convergence and does *not* utilize (or require) knowing the asymptotic sum as defined above. This technique is described in Appendix B, and with it the accuracy is improved to one part in 10^6 and increases by a factor of about 3.36 as each additional term is added to the sum. In this way, we find that

$$f_0(0, 1) = 1.000\,000\,2 \pm 8 \,.$$

The $\pm$ quantities are the bounds on the exact value, *not* statistical uncertainties (e.g., from roundoff errors, etc.). Returning to the dipole case, the asymptotic value of $f_{\rm crit}$ is then

$$f_{\rm crit} \approx -(\pi^2/\sqrt{2}) \sum_{n=1}^{\infty} (-1)^n n = \pi^2/\sqrt{32} \,, \tag{43}$$

whereas our estimate by forcing convergence of the actual series, given from table A2 in the Appendix, is

$$f_{\rm crit} = 1.591\,842\,8 \pm 4 \,. \tag{44}$$

In our notation, f is also proportional to the magnetic flux; and for an unperturbed dipole, $f_1(0, 1) = 1$. Thus the effect of the field-line deformation is to increase the

magnetic flux that extends through the light cylinder by more than 60 percent, and the magnetic energy density near the light cylinder is increased by more nearly a factor of $(1.59)^2 = 2.53$. Another way of viewing $f_{\rm crit}$ is to note that the field line that would have closed at $\rho = 1/f_{\rm crit} = 0.628\ldots$, were there no rotation, is the one that now is distorted to form the cusp.

It is interesting to note that if we correct the asymptotic value of $f_{\rm crit}$ by renormalizing it against the asymptotic value for f_0, then

$$f_{\rm crit} \approx f_1(\text{asymp.})/f_0(\text{asymp.}) = \pi/2 = 1.570\ldots, \tag{45}$$

and we would have come within about 1 percent of the exact value. This fact suggests the approximation in the next section. Table B2 in the Appendix lists the first few values of f_k derived from the series and compares them with that estimated by "normalizing" the asymptotic values as in expression (45) above.

VI. APPROXIMATE EXPRESSION FOR $f_1(z, \rho)$ NEAR LIGHT CYLINDER

Since (see Appendix A)

$$\psi_n(\rho) \approx \text{const.} \times J_0(\lambda_n(1 - \rho)) \qquad \text{as } \rho \to 1\,, \tag{46}$$

we can use the integral representation for J_0 and the approximation $\lambda_n \to n\pi$ to write

$$f_0(z, \rho) \approx \frac{1}{\pi} \operatorname{Re} \int_0^{2\pi} d\theta \sum \exp\left[-n\pi z + in\pi(1 - \rho)\sin\theta\right](-1)^n \tag{47}$$

$$\approx \frac{1}{\pi} \operatorname{Re} \int_0^{2\pi} d\theta/\{1 + \exp\left[-\pi z + i\pi(1 - \rho)\sin\theta\right]\,. \tag{48}$$

The latter integral must itself be approximated, which we do by expanding about $\rho = 1$ to obtain

$$f_0(\text{approx.}) = \frac{1}{\pi} \operatorname{Re} \int_0^{2\pi} d\theta/(a + ib\sin\theta)\,, \tag{49}$$

where $a = 1 + e^{-\pi z}$ and $b = e^{-\pi z}\pi(1 - \rho)$. Taking the real part then gives

$$f_0(\text{approx.}) = \frac{1}{\pi} \int_0^{2\pi} a d\theta/(a^2 + b^2\sin^2\theta)\,, \tag{50}$$

which integrates to give

$$f_0(\text{approx.}) = 2/(a^2 + b^2)^{1/2} \tag{51}$$

$$= 2(1 + 2e^{-\pi z} + e^{-2\pi z}[1 + \pi^2(1 - \rho)^2])^{-1/2}\,. \tag{52}$$

VII. MAGNETIC FIELD STRENGTH AT THE LIGHT CYLINDER

The field lines cross the light cylinder normally, and in a section dz of the light cylinder passes a flux $d\Phi = 2\pi(\partial f/\partial z)_{\rho=1}dz$; hence the magnetic field strength is given by

$$B = \left(\frac{\partial f}{\partial z}\right)_{\rho=1}\,. \tag{53}$$

Thus for the dipole case,

$$B_1(z) = \sum w_n\lambda_n^2 \exp\left(-\lambda_n z\right)\psi_n(1)\,, \tag{54}$$

and in general we see that, at the light cylinder,

$$B_k(z) = \pm f_{k+1}(z, 1)\,, \tag{55}$$

which also follows immediately from equation (12a). The asymptotic series at $z = 0$ is proportional to $\sum (-1)^n n^2$ whose Abel sum is zero. The exact series also sums to zero under forced convergence. That the field is zero follows physically from the fact that it must be at such a cusp. The field strength then rises to a maximum (near $z = 0.42$) and soon declines exponentially [$\approx \exp(-\lambda_1 z)$ with $\lambda_1 = 3.22$], as do the charge density, current density, and electric field.

VIII. CHARGE DENSITY AT THE CUSP OF THE LIGHT CYLINDER

From equation (13) we have, at $\rho = 1$,

$$\mu_0 j_0 c = -(f_{\rho\rho} + f_{zz})/\rho\,, \tag{56}$$

and from equation (24) we then obtain quantities

$$j_0 = -f_{zz}/2\mu_0 c\,; \tag{57}$$

however, here f is that appropriate for a dipole, hence

$$j_0 = -f_3/2\mu_0 c \qquad \text{(cusp)}\,. \tag{58}$$

Putting dimensions back into the equation and writing f in terms of the polar (dipole) magnetic field (B_p) at the surface of an object with radius a, we obtain

$$j_0 = -\tfrac{1}{4} f_3(0, 1)\epsilon_0 \omega B_p (\omega a/c)^3 \qquad \text{(cusp)}\,. \tag{59}$$

For a pulsar with a 3-second period ($\omega \approx 1$ rad s^{-1}) and the usually assumed neutron-star size and field ($a = 10$ km, $B_p = 10^{12}$ gauss), we obtain $j_0 \approx 1.2 \times 10^3$ electron charge per m^3. To explain coherence of the radiofrequency radiation, one must have all the electrons more together over a scale size of meters, and the above ambient charge density could therefore provide only a coherence factor of about 10^3. Thus if the pulsar radiation came from electron bunches of order 10^{10} per m^3 slung around near the light cylinder (Gold 1968), these bunches would create currents far in excess of that required to open the field lines. Our axisymmetric treatment does not permit us to calculate directly any limits on possible particle bunching, although it might be possible to do a linearized stability treatment to look for an instability that might cause bunching. However, one can make the plausibility argument that the local magnetic field generated by the motion of such a bunch itself does not exceed the ambient magnetic field. In this way we can locate how far inward from the cusp that such a bunch would have to be to corotate and yet be confirmed by the magnetic field of the rotator. But this distance is relatively large since the field is zero at the cusp; moreover, the Lorentz factor varies as

$$\gamma = (1 - \rho^2)^{-1/2} \approx (2 - 2\rho)^{-1/2} \qquad \text{as } \rho \to 1\,. \tag{60}$$

The brightness temperature of such a radiating bunch is given roughly by

$$T_B \approx 6 \times 10^9 N(\gamma - 1)^\circ \text{ K}\,; \tag{61}$$

and for $\omega = 1$ rad s^{-1} pulsar with a bunch no closer than 1 meter from the light cylinder, we have $\gamma = 10^4$, hence require $N \approx 10^{10}$. But these concentrations are so large that certainly $(\gamma - 1) \approx \frac{1}{2}\rho^2 \approx$ order unity, which in turn requires $N \approx 10^{14}$

or more, and the luminosity of such transrelativistic particles would be too low (by a factor of around 10^8) to be interesting as a pulsar radiation source.

IX. DISCUSSION

If the particle inertia had not been neglected, one would feel comfortable in interpreting the field-line configuration shown in figure 1*b* as representing field lines "pulled open" by centrifugal forces. But even without direct particle inertia, the magnetic field itself has energy and momentum. Without the plasma introducing the $\boldsymbol{E} + \boldsymbol{V} \times \boldsymbol{B} = 0$ condition, the magnetic field would be static. In the plasma, one has a "rotating" magnetic field (i.e., the associated electrostatic field, with E/B interpreted as the rotational velocity). There is therefore a nonvanishing Poynting vector $\boldsymbol{S} = \boldsymbol{E} \times \boldsymbol{B}$ and furthermore a nonvanishing angular momentum density $\boldsymbol{M} = \boldsymbol{r} \times \boldsymbol{S}$. It is easy to see that ultimately one has a local Poynting vector flux which exceeds that which could be supplied by the local energy density being transported at the velocity of light. In other words, the field lines are pulled open by the centrifugal force exerted by the corotating energy density in the electromagnetic fields, even if the particles do not themselves contribute a centrifugal force. (I am indebted to D. Rayburn, who had made rough estimates using such a view, for pointing out the role of effective field inertia to me.) An entirely equivalent view is simply that the electrostatic repulsion of the charged field lines acts to blow them open. The role of the particle inertia, which of course is not zero in reality, is probably easier to appreciate in the former picture, however.

Clearly it is desirable next to include particle inertia; however, introduction of finite particle masses introduces *two* problems: (1) the inertial effects of the particles themselves, and (2) flow of the plasma along the open field lines. The first factor is probably relatively straightforward to deal with, but the second requires additional important auxiliary assumptions regarding the equation of state for the plasma. Of particular interest would be to extend these solutions to the nonaxisymmetric case. It is hoped that the existence of a detailed qualitative model will encourage further work on the physics of rotating magnetized objects. Working FORTRAN programs for the calculation of eigenstates, eigenfunctions, and forcing convergence of the eigenvalue expansion series are available on request. Possibly a limited number of punched decks can be provided.

I am indeed indebted to Carl Kaysen, Director of the Institute for Advanced Study where this work was initiated, for his hospitality, and to Sir Fred Hoyle, Director of the Institute of Theoretical Astronomy where this work was completed. The stimulating atmospheres provided at these two fine institutes was instrumental in helping the author overcome several "potential barriers" encountered in the course of this work. The work was supported in part by NSF grant GP-25854.

APPENDIX A

THE LIGHT-CYLINDER EQUATION

The differential equation

$$\psi_{xx} - \frac{1}{x}\left(\frac{1 + x^2}{1 - x^2}\right)\psi_x + \lambda^2\psi = 0 \tag{A1}$$

is quite similar to the Mathieu equation in terms of its singularities, which are at

$x = 0, \pm 1$, and $\pm\infty$. These five singularities can be reduced to three by the substitution $z = x^2$ which yields

$$\psi_{zz} + \frac{1}{z-1}\psi_z + \frac{\lambda^2}{4z}\psi = 0 . \tag{A2}$$

Thus we have two regular singularities at $z = 0, 1$ and an irregular singularity at infinity. Returning to equation (A1), we can write it in the form

$$(g\psi_x)_x + \lambda^2 g\psi = 0 , \tag{A3}$$

where

$$g = (1 - x^2)/x . \tag{A4}$$

Accordingly, we can define the conjugate function ϕ where

$$\phi = g\psi_x/\lambda \tag{A5}$$

and

$$\phi_x = -\lambda g\psi ; \tag{A6}$$

thus,

$$(g^{-1}\phi_x)_x + \lambda^2 g^{-1}\phi = 0 , \tag{A7}$$

and therefore ϕ satisfies the same differential equation as ψ except that the sign of the second term (in A1) is reversed.

The eigenstates of equation (A1) are at the values of λ^2 for which $\psi_x(1) = 0$ [$\psi(1)$ finite], which we number consecutively from one (the "first" eigenstate). These eigenstates are all distinct, and the eigenfunctions satisfy the orthogonality relations

$$\int_0^1 \psi_n\psi_m g dx = 0 \qquad (n \neq m) \tag{A8}$$

and

$$\int_0^1 \phi_n\phi_m g^{-1} dx = 0 \qquad (n \neq m) . \tag{A9}$$

One can also show, integrating by parts, that the normalization integrals are related by

$$\int_0^1 \psi_n{}^2 g dx = \int_0^1 \phi_n{}^2 g^{-1} dx \equiv h_n , \tag{A10}$$

but we have no expression for h_n in terms of ϕ_n, ψ_n, or their differentials. One useful relation that follows directly from equation (A6) is

$$\int_0^1 \psi_n g dx = +\phi_n(0)/\lambda_n , \tag{A11}$$

which we use in the text (eq. [35]).

a) Power-Series Expansion

If ψ and ϕ are to be finite in the interval [0, 1], they must be even functions of x; thus

$$\psi(x) = \psi(-x) \tag{A12}$$

and

$$\phi(x) = \phi(-x)\,. \tag{A13}$$

Hence we write

$$\psi(x) = \sum_{k=1}^{\infty} a_k x^{2k}\,, \tag{A14}$$

$$\phi(x) = \sum_{k=0}^{\infty} b_k x^{2k}\,, \tag{A15}$$

and obtain the three-term recursion relations

$$4k(k+1)a_{k+1} + (\lambda^2 - 4k^2)a_k - \lambda^2 a_{k-1} = 0\,, \tag{A16}$$

$$4(k+1)^2 b_{k+1} + (\lambda^2 - 4k(k-1))b_k - \lambda^2 b_{k-1} = 0\,, \tag{A17}$$

the first nonzero terms being a_1 and b_0. From these and the relation (5) or (6) between ψ and ϕ we find

$$2a_1 = \lambda b_0\,. \tag{A18}$$

Figures 2 and 3 show the first three (unnormalized) eigenfunctions plotted for the choice $a_1 = 1$. Equation (A18) is equivalent to

$$\lambda\phi(0) = \psi_{xx}(0) \tag{A19}$$

and

$$\phi_{xx}(0) = -\lambda^2\phi(0)/2\,, \tag{A20}$$

etc. Similar relations follow for values at $x = 1$. Note that ϕ diverges while ψ converges for $x \to \infty$ in figures 2 and 3.

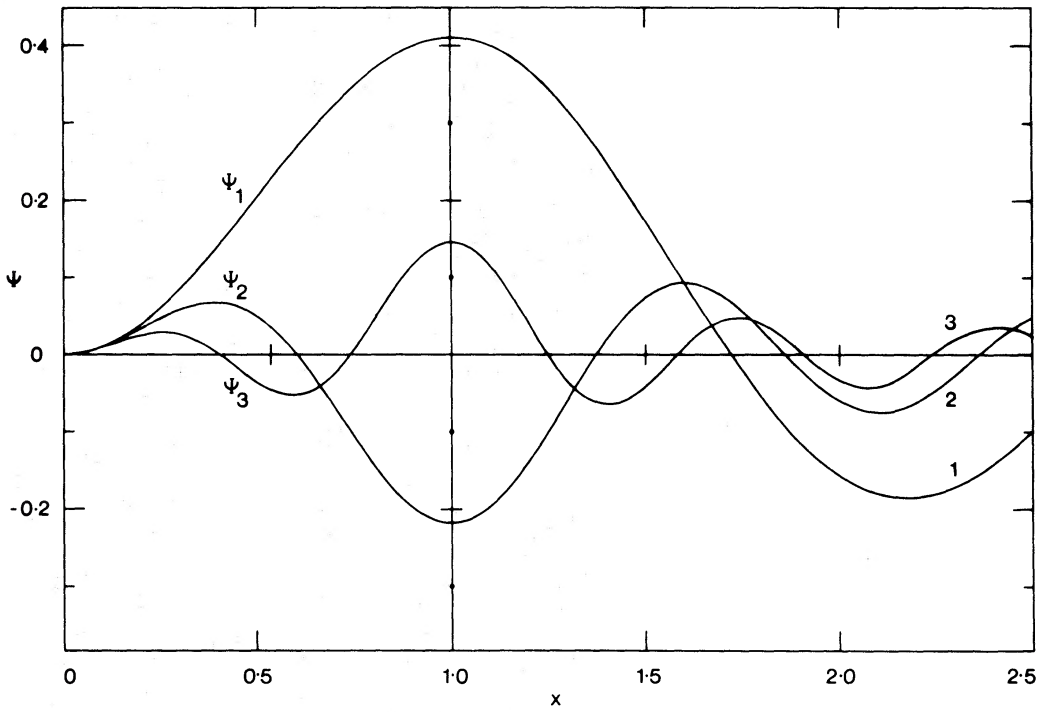

FIG. 2.—Computer plots of the functions ψ_n for $n = 1$, 2, and 3, normalized to fixed $\psi_n''(0)$

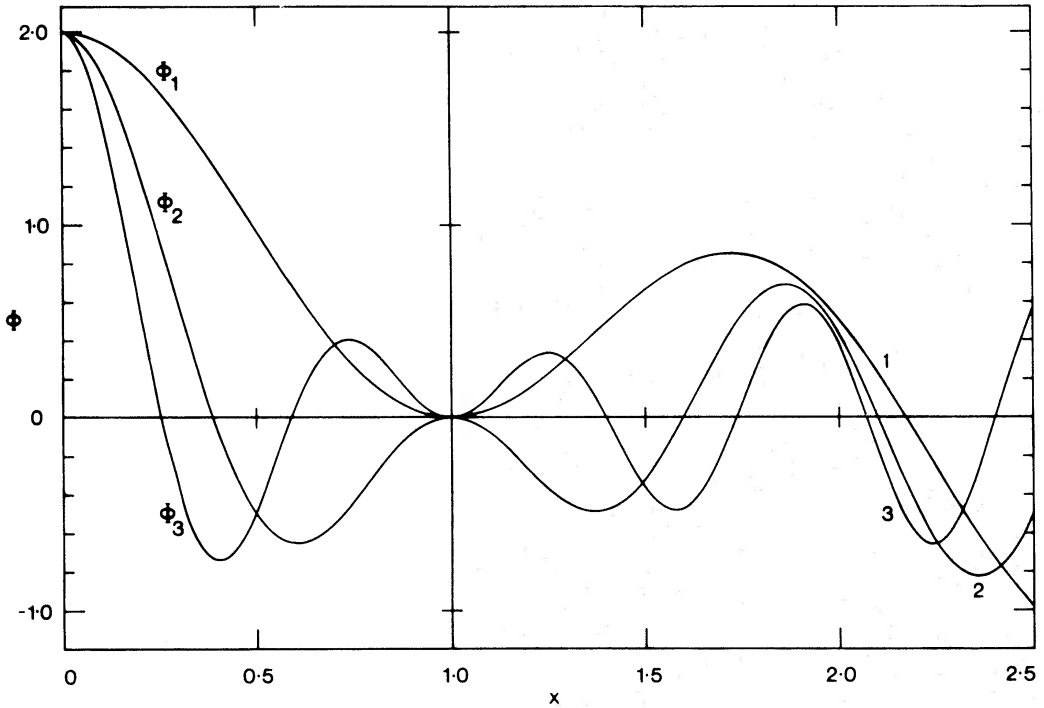

FIG. 3.—Computer plots of the functions ϕ_n for $n = 1$, 2, and 3, normalized to fixed $\phi_n(0)$

b) Eigenvalues

From figure 2 we see that the eigenstates are oscillating functions, the nth eigenstate having $n - 1$ zeros. It is clear, then, that for large λ_n the oscillating behavior dominates; hence

$$\lambda_n \to n\pi \qquad \text{as } n \to \infty \,, \tag{A21}$$

since ψ_x is of order λ_n while ψ_{xx} and $\lambda^2\psi$ are both of order $\lambda_n{}^2$ and therefore dominate.

The eigenstates can be determined from the recursion formula (A14). The divergence at $x = 1$ (except for the eigenstates) is revealed in the recursion relation by the behavior

$$a_{k+1} \to a_k \qquad \text{as } k \to \infty \,, \tag{A22}$$

in which case the sum does not converge on the unit circle unless $a_k \to 0$. The eigenvalue behavior is that the a_k alternate in sign and increase in magnitude up to $k \approx \lambda/2$, thereafter declining exponentially to zero. The expansion coefficients for the first three eigenstates are given in table A1. The eigenstates were determined simply by iterating to drive some sufficiently large coefficient (a_{100}, say) to essentially zero. Roundoff errors prevent that value from being zero, and the method is thereby limited to the first few eigenstates. Table A1 is the result of calculations to 10 significant places.

The recursion relation (A14) can be rewritten as the continued fraction

$$\alpha = 1 - \cfrac{2\alpha}{\alpha - 4 + \cfrac{2\cdot 3\alpha}{\alpha - 9 + \cdots + \cfrac{N_n}{D_n + \cdots}}} \tag{A23}$$

TABLE A1

EXPANSION COEFFICIENTS

λ_1^2	10.365 287 46[5]
a_k, $k = 1$	1
2	−0.795 660 933
3	+0.245 081 951
4	−0.040 930 186
5	+0.004 313 326
6	−0.000 313 578
7	+0.000 016 690
8	−0.000 000 679
9	+0.000 000 022
10	−0.000 000 001
$\psi_n(1.0)$	0.412 506 613
h_n	0.038 619 261

NOTE.—The first coefficient a_1 is normalized to unity.

where $\alpha = \lambda^2/4$, $N_n = n(n-1)\alpha$, and $D_n = \alpha - n^2$. If one writes equation (A23) in the form

$$\alpha_{j+1} = \text{continued fraction } (\alpha_j) \tag{A24}$$

and iterates, one finds that such a procedure converges on the odd eigenstates. Convergence can be obtained on the even eigenstates by using $2\alpha_j - \alpha_{j+1}$ for the next guess instead of α_{j+1}. Substantially the same difficulty from roundoff errors is encountered here as in the recursion relation calculations: one loses about one place of significance in each succeeding eigenvalue for calculations done to a fixed number of places.

The most satisfactory approach ultimately was simply to integrate the differential equations (A1), (A2) or (A5), (A6) numerically and iterate to find the eigenvalue to satisfy the boundary conditions. Table A2 shows the results of double-precision calculations to determine eigenfunctions to seven significant places (single precision). The eigenfunctions were computed by a Runge-Kutta routine in steps of 0.001.

c) *Asymptotic Expressions*

If the eigenvalue λ_n is large, ψ_n becomes a rapidly oscillating function, in which case we can contemplate the approximation

$$\psi_n(x) \to f_n(x) \cos(\lambda_n x + \eta) \qquad \text{as } n \to \infty . \tag{A25}$$

Terms of order λ_n^2 cancel in equation (A3), and setting the coefficient terms of order λ_n equal to zero gives

$$f_n(x) = K_n/g(x)^{1/2} , \tag{A26}$$

where the constant K_n is undetermined, as well as the phase factor η. For Bessel's equation $g = x$ and we obtain the standard form of the asymptotic expansion (large x). The normalization integral (A10) then becomes

$$h_n = \int_0^1 \psi_n^2 g dx \approx K_n^2/2 , \tag{A27}$$

and our problem then reduces to determining K_n. But we know that for $x \to 1$,

TABLE A2

COMPUTED VALUES, RESPECTIVELY, AS A FUNCTION OF n, FOR THE EIGENVALUE, THE EIGENVALUE EXPANSION TERMS FOR $f_0(0, 1)$, THE LAST VALUE OF ψ_n, AND THE NORMALIZATION INTEGRAL

A

n	λ_n	$\phi_n(0)\psi_n(1)/\lambda_n h_n$
1.....	3.219 517	2.060 988 627
2.....	6.336 203	−2.140 969 193
3.....	9.765 611	2.168 766 081
4.....	12.599 901	−2.182 555 357
5.....	15.736 585	2.190 719 318
6.....	18.874 629	−2.196 092 762
7.....	22.013 523	2.199 887 918
8.....	25.152 988	−2.202 706 425
9.....	28.292 855	2.204 880 122
10.....	31.433 018	−2.206 606 191

B

	$\psi_n(1)$	h_n
1.....	+0.412 506 589	0.038 619 256 ...
2.....	−0.216 234 827	0.005 031 379 ...
3.....	+0.146 286 974	0.001 505 655 6.
4.....	−0.110 481 468	0.000 637 705 06.
5.....	+0.088 741 285	0.000 327 150 87.
6.....	−0.074 144 017	0.000 189 539 06.
7.....	+0.063 667 821	0.000 119 445 68.
8.....	−0.055 784 128	0.000 080 058 037
9.....	+0.049 636 903	0.000 056 246 589
10.....	−0.044 709 522	0.000 041 014 089

NOTE.—The numerically computed eigenvalues differ slightly in the last place from those more accurately calculated by the continued-fraction method, owing to finite-difference and roundoff limitations.

equation (A1) becomes Bessel's equation if we write $z = 1 - x$ and therefore

$$\psi_n(x) \to \psi_n(1) J_0(\lambda_n z) \qquad \text{as } x \to 1 . \tag{A28}$$

Since the asymptotic expansion for (A28) is

$$\psi_n(x) \to \psi_n(1)(2/\pi\lambda_n z)^{1/2} \cos(\lambda_n z - \tfrac{1}{4}\pi) , \tag{A29}$$

comparison with (A25) and (A26), noting that $g \to 2z$, then gives us

$$\eta \to -\pi/4 , \tag{A30}$$

$$K_n \to 2\psi_n(1)/(\pi\lambda_n)^{1/2} ; \tag{A31}$$

and as noted before,

$$\lambda_n \to n\pi .$$

Thus a convenient normalization is to set $h_n = 1$, whence

$$\psi_n(1) = (\pi\lambda_n/2)^{1/2} \qquad (h_n \to 1 \text{ as } n \to \infty) ; \tag{A32}$$

and finally

$$\psi_n(x) = (2/g)^{1/2} \cos(n\pi x - n\pi - \tfrac{1}{4}\pi) \qquad (1/n \ll x \ll 1 - 1/n)\,. \tag{A33}$$

At the other limit, $x \to 0$, we have Bessel's equation except the sign of the first derivative term is negative; thus the solution is

$$\psi_n(x) \to \psi_n''(0) x J_1(\lambda_n x)/\lambda_n \qquad \text{as } x \to 0\,, \tag{A34}$$

which we have normalized as above since both ψ_n and its first derivative are zero. Equation (A34) has the asymptotic limit

$$\psi_n(x) \to \psi_n''(0)(2x/\pi\lambda_n^3)^{1/2} \cos(n\pi x - \pi - \tfrac{1}{4}\pi)\,, \tag{A35}$$

and equating (A35) with (A33) gives as $x \to 0$

$$\psi_n''(0) = -\cos(n\pi)(\pi\lambda_n^3)^{1/2}\,. \tag{A36}$$

We note that $\phi_n(0)$ is given from equation (A19) to be

$$\phi_n(0) = \psi_n''(0)/\lambda_n = (-1)^n(\pi\lambda_n)^{1/2}\,. \tag{A37}$$

Since $\phi_n(x)$ satisfies Bessel's equation as $x \to 0$, we then obtain

$$\phi_n(x) \to \phi_n(0) J_0(\lambda_n x) \qquad \text{as } x \to 0\,, \tag{A38}$$

and, as for ψ_n,

$$\phi_n(x) \approx (-1)^n(2g)^{1/2} \cos(n\pi x - \tfrac{1}{4}\pi)\,. \tag{A39}$$

It follows then that the normalization integral

$$\int_0^1 \phi_n^2 g^{-1} dx \to 1 \qquad \text{as } n \to \infty \tag{A40}$$

is in agreement with (A10). From (A37) we finally obtain

$$\psi_n(1)/\phi_n(0) \to (-1)^n/\sqrt{2} \qquad \text{as } n \to \infty\,. \tag{A41}$$

APPENDIX B

CONVERGENCE WEIGHTING TECHNIQUE

Consider the series

$$S = \sum_{n=0}^{\infty} (-1)^n = 1 - 1 + 1 - 1 + 1 - 1 + \cdots, \tag{B1}$$

which can be summed using

$$(1 + x)^{-1} = \sum_{n=0}^{\infty} (-1)^n x^n\,; \tag{B2}$$

thus

$$S = \lim_{x \to 1} (1 + x)^{-1} = \tfrac{1}{2}\,, \tag{B3}$$

which is mathematically unacceptable. However, if we know that the series S is only approximate and that the higher-order terms ultimately decrease to zero, then the approach is justified. But what if the terms start off as ± 1, *grow* to ± 2, and then ultimately decrease to zero? How then can the series be estimated? A clue may be obtained from the partial sums S_N of S, where

$$S_N = \sum_{n=0}^{N} (-1)^n = \sum a_n \,. \tag{B4}$$

These values alternate 0 and 1 and oscillate about the value of $\frac{1}{2}$. A more rapid convergence is obtained if we define a new (weighted) partial sum

$$A_N = (S_N + S_{N-1})/2 \,. \tag{B5}$$

Thus

$$\lim_{N\to\infty} A_N = S \tag{B6}$$

and

$$A_N = S_N - \tfrac{1}{2}a_N \,. \tag{B7}$$

With regard to series (B1), we see that

$$A_N = \tfrac{1}{2} \qquad \text{for all } N \geq 1 \,. \tag{B8}$$

Indeed, the series is summed immediately using only the first term! Table B1 shows the behavior of A_N as N increases from 1 to 10. It will be noted there that the improvement gained by adding each additional terms starts to decline noticeably. However, one also notices that they themselves oscillate about the exact value; thus why not apply the same trick twice—namely, define a weighted partial sum [we now regard A_N as being $A_N(1)$]

$$A_N(2) = (A_N(1) + A_{N-1}(1))/2 \,, \tag{B9}$$

which we have also listed in table B1? One notes first that $A_2(2)$ is actually a slightly *inferior* estimate to $A_2(1)$, but improves and by the tenth term the exact value is given within 0.000 046, a tenfold improvement over $A_{10}(1)$. But $A_N(2)$ itself oscillates about

TABLE B1

WEIGHTED PARTIAL SUMS OF ORDER 1 AND 2 FOR THE SERIES $\phi_n(0)\psi_n(1)/h_n\lambda_n$ IN TABLE A2 VERSUS NUMBER OF TERMS (N) USED IN TRUNCATED SERIES

N (or m)	$A_N(1) - 1$	$A_N(2) - 1$	$A_{10}(m) - 1$
1.....	+0.030 494 313	(undefined)	−0.000 384 768
2.....	−0.009 495 969	+0.010 499 171	+0.000 046 749
3.....	+0.004 402 474	−0.002 546 747	−0.000 009 204
4.....	−0.002 492 163	+0.000 955 155	+0.000 003 119
5.....	+0.001 589 817	−0.000 451 172	−0.000 001 087
6.....	−0.001 096 905	+0.000 246 456	+0.000 001 023
7.....	+0.000 800 672	−0.000 148 116	−0.000 000 582
8.....	−0.000 608 581	+0.000 096 045	+0.000 001 236
9.....	+0.000 478 266	−0.000 065 157	−0.000 002 232
10.....	−0.000 384 768	+0.000 046 749	+0.000 010 084

NOTE.—In the last column is instead the weighted partial sum of order m using 10 terms. Thus $A_{10}(1)$ and $A_{10}(2)$ appear twice.

the exact value, and we can once more define a new partial sum to take advantage of that oscillation. Indeed in general we can define the mth-weighted partial sum

$$A_N(m) = (A_N(m-1) + A_{N-1}(m-1))/2 \qquad (m \leq N)\,. \tag{B10}$$

However, it does not follow that the tenth weighted partial sum is the closest to the exact value, as can be seen by calculating succeeding partial sums for, say, $N = 10$ as are shown in table B1. There we note that $m = 7$ happens to give the closest estimate, coming within 0.000 000 583 of the exact value. One finds in fact that the best weighted partial sum for a given N is improved by better than a factor of 3 as each new term is added, thus an order of magnitude with every pair of terms. (On a log-linear plot, these deviations fall extraordinarily close to a straight line.) Clearly we will rapidly come to the point where the terms themselves are not known to sufficient accuracy to provide further improvement.

We must stress that it is not necessary to know the sum in advance to know which is the best weighted partial sum, because the differences between successive weighted partial sums themselves oscillate about the correct value, and it is only necessary to choose the two closest successive values to obtain an upper and lower bound to the correct value. It is clear that sums such as

$$f_1(z, \rho) = \sum \phi_n(0) \exp(-\lambda_n z)\psi_n(\rho)/h_n$$

can, by using the weighting techniques to accelerate convergence on the 10 terms listed in table A2, be used to calculate f_1 at any point and thereby form a plot of the field lines. Indeed, it was in this way that the plotted points in figures 1*a* and 1*b* are obtained. Table B2 tabulates the first few values of $f_k(0, 1)$.

After some search, we have discovered that exactly the same method was discovered by Hutton (1812), but seems not to have found its way into modern textbooks on mathematical physics. The reader concerned over the mathematical acceptability of such summation techniques when applied to divergent series is referred to the comprehensive discussion by Hardy (1949).

TABLE B2

VALUES OF $f_k = (-1)^k(\partial^k f_0/\partial z_k)$ EVALUATED AT THE CUSP POINT $z = 0$, $\rho = 1$ AS CALCULATED FROM FORCED CONVERGENCE OF THE EIGENVALUE EXPANSION (10 terms) AND COMPARED WITH THE NORMALIZED ASYMPTOTIC VALUES

k	f_k(series)	f_k(asymp.)/f_0(asymp.)
0	1.000 000 2 ± 8	1 (by definition)
1	1.591 842 8 ± 4	$\pi/2 = 1.570\ldots$
2	0.000 04 ± 8	0 (exact)
3	8.017 6 ± 1	$\pi^3/4 = 7.751\ldots$
4	0.001 ± 2*	0 (exact)
5	160.4 ± 1*	$\pi^5/2 = 153.009\ldots$
6	1 ± 2*	0 (exact)
7	6850 ± 20*	$17\pi^7/8 = 6418.123\ldots$
8	Requires more terms*	0 (exact)

* Roundoff errors are also entering in these higher-order terms, and therefore these variances are no longer bounds but also contain a statistical component. The variances refer, of course, to the *least* significant figures; thus 0.001 ± 2 means 0.001 ± 0.002, etc.

REFERENCES

Ferraro, 1937, *M.N.R.A.S.*, **97**, 458.
Gold, T. 1968, *Nature*, **218**, 731.
Hardy, G. H. 1949, *Divergent Series* (Oxford: Oxford University Press).
Hutton, C. 1812, *Tracts on Mathematical and Philosophical Subjects* (London: Wilkie & Robinson, Booksellers), **1**, 176 *et seq.*
Michel, F. C. 1969, *Ap. J.*, **158**, 727.